Coexistence of s- and d-wave gaps due to pair-hopping and exchange interactions

E-mail: shigeami@secondlab.co.jp

Shigeru Koikegami

Second Lab, LLC, 19-27 Inarimae, Tsukuba 305-0061, Japan

Abstract. I investigate the superconductivity of the three-band t–J–U model derived from the three-band Hubbard model using the Schrieffer–Wolff transformation. My model is designed considering the hole-doped high-T_c superconducting cuprate. The model does not exclude the double occupancy of Cu sites by d electrons, and there is a pair-hopping interaction between the d and p bands together with the exchange interaction. I analyse the superconducting transition temperature, electronic state, and superconducting gap function based on strong coupling theory and find that the superconductivity emerges due to the pair-hopping and exchange interactions via the Suhl-Kondo mechanism. In the superconducting state, the extended s- and $d_{x^2-y^2}$-wave superconducting gaps coexist, where both charge fluctuations and d–p band hybridization are key ingredients.

1. Introduction

The t–J model is one of the model Hamiltonians that form the basis of many theoretical studies of strongly correlated electron systems [1, 2]. The t–J model can also be derived as the low-energy effective Hamiltonian of the two-dimensional (2D) multiband Hubbard model [3–5], regarded as the fundamental model Hamiltonian for the high-T_c superconducting cuprate (HTSC). Many theoretical studies of HTSC to date use the t–J model as the model Hamiltonian [6–13]. These studies often exclude the double occupancy of Cu sites by d electrons, considering that the on-site Coulomb repulsion between d orbitals is much larger than the transfer energy between the d and p orbitals. As a result, the t–J model contains only one electron (or hole) band and a localized spin.

However, the double occupancy of Cu sites need not necessarily be excluded when the on-site Coulomb repulsion U is comparable to the transfer energy. Relaxing the single occupancy constraint and explicitly considering U instead results in the t–J–U model that includes both the t–J model and the single-band Hubbard model as one of its limits [14–20]. Thus, the t–J–U model serves as an interpolation between the t–J model and the single-band Hubbard model and is able to account for more properties

caused by strong correlation. However, the charge transfer gap should be comparable to t in the charge transfer regime. In this case, p electron scattering by d electrons cannot be negligible, and both p and d electrons must be considered.

In this paper, I derive the three-band t–J–U model from the 2D three-band Hubbard model as its effective Hamiltonian by using the Schrieffer–Wolff (SW) transformation [21] and assume that double occupancy is not excluded. In my model, the pair-hopping interaction between the d and p bands exists separately from the exchange interaction. Treating these interactions using iterative perturbation theory (IPT) approximation, I investigate the superconductivity of the model in a strong coupling framework. The results show that the multicomponent superconductivity emerges with the hole doping, which introduces the d-p band hybridization through exchange and pair-hopping interactions. This emergence of the superconductivity is due to the pair-hopping and exchange interactions via the Suhl-Kondo (SK) mechanism [22–24], which stabilizes the superconducting gaps with different signs in a multiband system. In the superconducting state, the extended s- and $d_{x^2-y^2}$-wave superconducting gaps coexist, and the s- and d-wave gaps emerge due to the pair-hopping and exchange interactions, respectively.

2. Formulation

Consider the three-band Hubbard model [25] that expresses the Hamiltonian as $\mathcal{H} = \mathcal{H}_0 + \sum_\alpha \mathcal{H}_1^\alpha$, where

$$\mathcal{H}_0 = \varepsilon_d \sum_{j\sigma} d_{j\sigma}^\dagger d_{j\sigma} + \varepsilon_p \sum_\alpha \sum_{\mathbf{k}\sigma} p_{\mathbf{k}\sigma}^{\alpha\dagger} p_{\mathbf{k}\sigma}^\alpha + U \sum_j d_{j\uparrow}^\dagger d_{j\uparrow} d_{j\downarrow}^\dagger d_{j\downarrow} \tag{1}$$

and

$$\mathcal{H}_1^\alpha = \frac{1}{\sqrt{N}} \sum_j \sum_{\mathbf{k}\sigma} \left(V_{\alpha\mathbf{k}} e^{-i\mathbf{k}\cdot\mathbf{R}_j} p_{\mathbf{k}\sigma}^{\alpha\dagger} d_{j\sigma} + \text{H.c.} \right). \tag{2}$$

Here, $\alpha \in \{x, y\}$; $d_{j\sigma}(d_{j\sigma}^\dagger)$ is the annihilation (creation) operator for the d electron of spin σ at Cu site j; $p_{\mathbf{k}\sigma}^\alpha(p_{\mathbf{k}\sigma}^{\alpha\dagger})$ is the annihilation (creation) operator for p^α electrons of spin σ with momentum $\mathbf{k}$, based on oxygen sites in real space; ε_d and ε_p are the d and p electron site energies, respectively; U is the on-site Coulomb repulsion between d orbitals; and N is the number of k-space points in the first Brillouin zone (FBZ). The lattice constant of the square lattice of Cu sites is the length unit. Thus, $V_{x\mathbf{k}} = 2it_{pd}\sin\frac{k_x}{2}$ and $V_{y\mathbf{k}} = -2it_{pd}\sin\frac{k_y}{2}$, where t_{pd} is the transfer energy between the d orbital and the neighbouring p^α orbital.

In order to derive the effective Hamiltonian for $\mathcal{H}$, I adopt the SW transformation as follows:

$$e^{\sum_\alpha \mathcal{S}^\alpha} \mathcal{H} e^{-\sum_\beta \mathcal{S}^\beta} = \mathcal{H}_0 + \sum_\alpha \mathcal{H}_1^\alpha + \sum_\alpha [\mathcal{S}^\alpha, \mathcal{H}_0] + \sum_{\alpha\beta} \left[\mathcal{S}^\alpha, \mathcal{H}_1^\beta\right] + \frac{1}{2}\sum_{\alpha\beta} \left[\mathcal{S}^\alpha, \left[\mathcal{S}^\beta, \mathcal{H}_0\right]\right] + \dots$$

$$= \mathcal{H}_0 + \frac{1}{2}\sum_{\alpha\beta} \left[\mathcal{S}^\alpha, \mathcal{H}_1^\beta\right] + \dots, \tag{3}$$

using $\mathcal{H}_1^\alpha + [\mathcal{S}^\alpha, \mathcal{H}_0] = 0$ and

$$\mathcal{S}^\alpha = \frac{1}{\sqrt{N}} \sum_j \sum_{\mathbf{k}\sigma} \left(\frac{V_{\alpha\mathbf{k}} e^{-i\mathbf{k}\cdot\mathbf{R}_j}}{\Delta_{pd} - U} n_{dj-\sigma} p_{\mathbf{k}\sigma}^{\alpha\dagger} d_{j\sigma} + \frac{V_{\alpha\mathbf{k}} e^{-i\mathbf{k}\cdot\mathbf{R}_j}}{\Delta_{pd}} (1 - n_{dj-\sigma}) p_{\mathbf{k}\sigma}^{\alpha\dagger} d_{j\sigma} \right) - \text{H.c.} \quad (4)$$

Here, $\Delta_{pd} \equiv \varepsilon_p - \varepsilon_d$, $n_{dj\sigma} \equiv d_{j\sigma}^\dagger d_{j\sigma}$, and H.c. indicates the Hermitian conjugate of the terms already written. The observable $n_{dj\sigma}$ has 0 or 1 as its eigenvalue for each j and σ. Using Eqs. (2) and (4), the following results:

$$
\begin{aligned}
\left[\mathcal{S}^\alpha, \mathcal{H}_1^\beta \right] = &-\frac{\delta_{\alpha\beta}}{N} \sum_{jj'} \sum_{\mathbf{k}\sigma} \left(\frac{n_{dj-\sigma}}{\Delta_{pd} - U} + \frac{1 - n_{dj-\sigma}}{\Delta_{pd}} \right) V_{\alpha\mathbf{k}} V_{\beta\mathbf{k}}^* e^{-i\mathbf{k}\cdot\mathbf{R}_j} e^{i\mathbf{k}\cdot\mathbf{R}_{j'}} d_{j'\sigma}^\dagger d_{j\sigma} \\
&+ \frac{1}{N} \sum_j \sum_{\mathbf{k}\mathbf{k}'\sigma} \left(\frac{n_{dj-\sigma}}{\Delta_{pd} - U} + \frac{1 - n_{dj-\sigma}}{\Delta_{pd}} \right) V_{\alpha\mathbf{k}} V_{\beta\mathbf{k}'}^* e^{-i\mathbf{k}\cdot\mathbf{R}_j} e^{i\mathbf{k}'\cdot\mathbf{R}_j} p_{\mathbf{k}\sigma}^{\alpha\dagger} p_{\mathbf{k}'\sigma}^\beta \\
&- \frac{1}{N} \sum_j \sum_{\mathbf{k}\mathbf{k}'\sigma} \left(\frac{1}{\Delta_{pd} - U} - \frac{1}{\Delta_{pd}} \right) V_{\alpha\mathbf{k}} V_{\beta\mathbf{k}'}^* e^{-i\mathbf{k}\cdot\mathbf{R}_j} e^{i\mathbf{k}'\cdot\mathbf{R}_j} p_{\mathbf{k}\sigma}^{\alpha\dagger} p_{\mathbf{k}'-\sigma}^\beta d_{j-\sigma}^\dagger d_{j\sigma} \\
&- \frac{1}{N} \sum_j \sum_{\mathbf{k}\mathbf{k}'\sigma} \left(\frac{1}{\Delta_{pd} - U} - \frac{1}{\Delta_{pd}} \right) V_{\alpha\mathbf{k}} V_{\beta\mathbf{k}'} e^{-i\mathbf{k}\cdot\mathbf{R}_j} e^{-i\mathbf{k}'\cdot\mathbf{R}_j} p_{\mathbf{k}\sigma}^{\alpha\dagger} p_{\mathbf{k}'-\sigma}^{\beta\dagger} d_{j-\sigma} d_{j\sigma} + \text{H.c.}
\end{aligned}
$$
$$(5)$$

Hereafter, I consider only the first two terms of the right-hand side of Eq. (3), i.e., up to the second order of t_{pd}. Now, I assume that the distribution of the d electron is spatially uniform in the ground state and that the ground state is paramagnetic. Thus, $\langle n_{dj\uparrow} + n_{dj\downarrow} \rangle_0 \equiv n_d$ and $\langle n_{dj\uparrow} \rangle_0 = \langle n_{dj\downarrow} \rangle_0$ for any j where n_d is a c-number equal to the number of d electrons in the ground state, where $\langle \cdots \rangle_0$ indicates the average in the ground state. I apply this approximation to Eqs. (3) and (5) and treat n_d as a parameter that should be determined self-consistently. When I set ε_p to zero, i.e., $\Delta_{pd} = -\varepsilon_d$, and omit the constant terms, I obtain the effective Hamiltonian:

$$\mathcal{H}_{\text{eff}} = \mathcal{H}_{\text{HF}} + \mathcal{H}_{\text{ex}} + \mathcal{H}_{\text{pair}} + \mathcal{H}_U'. \quad (6)$$

$\mathcal{H}_{\text{HF}}$ is the Hartree-Fock approximation of $\mathcal{H}_0$:

$$\mathcal{H}_{\text{HF}} = \sum_{\mathbf{k}\sigma} \varepsilon_{d\mathbf{k}} d_{\mathbf{k}\sigma}^\dagger d_{\mathbf{k}\sigma} + \sum_{\alpha\beta} \sum_{\mathbf{k}\sigma} \varepsilon_{\alpha\beta\mathbf{k}} p_{\mathbf{k}\sigma}^{\alpha\dagger} p_{\mathbf{k}\sigma}^\beta, \quad (7)$$

where $d_{\mathbf{k}\sigma}^\dagger = \frac{1}{\sqrt{N}} \sum_j d_{j\sigma}^\dagger e^{i\mathbf{k}\cdot\mathbf{R}_j}$, $d_{\mathbf{k}\sigma} = \frac{1}{\sqrt{N}} \sum_j d_{j\sigma} e^{-i\mathbf{k}\cdot\mathbf{R}_j}$,

$$\varepsilon_{d\mathbf{k}} = \varepsilon_d + \frac{U}{2} n_d + t \left(v_{x\mathbf{k}} v_{x\mathbf{k}}^* + v_{y\mathbf{k}} v_{y\mathbf{k}}^* \right), \quad (8)$$

and

$$\varepsilon_{\alpha\beta\mathbf{k}} = (Jn_d - t) v_{\alpha\mathbf{k}} v_{\beta\mathbf{k}}^*, \quad (9)$$

with $v_{x\mathbf{k}} = i \sin \frac{k_x}{2}$, $v_{y\mathbf{k}} = -i \sin \frac{k_y}{2}$,

$$t = 4 t_{pd}^2 \left(\frac{n_d}{\varepsilon_d + U} + \frac{1 - n_d}{\varepsilon_d} \right), \quad (10)$$

and

$$J = 2 t_{pd}^2 \left(\frac{1}{\varepsilon_d + U} - \frac{1}{\varepsilon_d} \right). \quad (11)$$

$\mathcal{H}_{\text{ex}}$ is an exchange interaction term:

$$\mathcal{H}_{\text{ex}} = \frac{J}{N} \sum_{\alpha\beta} \sum_{\mathbf{kk'}\sigma} \sum_{\mathbf{q}} v_{\alpha\mathbf{k}} v_{\beta\mathbf{k'}}^* p_{\mathbf{k}\sigma}^{\alpha\dagger} p_{\mathbf{k'}-\sigma}^{\beta} d_{\mathbf{k'}+\mathbf{q}-\sigma}^{\dagger} d_{\mathbf{k}+\mathbf{q}\sigma} + \text{H.c.} \tag{12}$$

$\mathcal{H}_{\text{pair}}$ is a pair-hopping term:

$$\mathcal{H}_{\text{pair}} = \frac{J}{N} \sum_{\alpha\beta} \sum_{\mathbf{kk'}\sigma} \sum_{\mathbf{q}} v_{\alpha\mathbf{k}} v_{\beta\mathbf{k'}} p_{\mathbf{k}\sigma}^{\alpha\dagger} p_{\mathbf{k'}-\sigma}^{\beta\dagger} d_{\mathbf{k'}-\mathbf{q}-\sigma} d_{\mathbf{k}+\mathbf{q}\sigma} + \text{H.c.} \tag{13}$$

$\mathcal{H}_U'$ is the Coulomb interaction term excluding the component with $\mathbf{q} = \mathbf{0}$:

$$\mathcal{H}_U' = \frac{U}{N} \sum_{\mathbf{kk'}} \sum_{\mathbf{q}\neq\mathbf{0}} d_{\mathbf{k}+\mathbf{q}\uparrow}^{\dagger} d_{\mathbf{k}\uparrow} d_{\mathbf{k'}-\mathbf{q}\downarrow}^{\dagger} d_{\mathbf{k'}\downarrow}. \tag{14}$$

As a consequence, $\mathcal{H}_{\text{eff}}$ [Eq. (6)] can be characterized by the three parameters t [Eq. (10)], J [Eq. (11)], and U, and it can be regarded as the three-band t–J–U model.

Here, t in Eq. (10) is positive near the half-filling in the charge-transfer regime, i.e., $U > -\varepsilon_d > 0$. For instance, in the case $\varepsilon_d = -U/2$, $t > 0$ for $n_d > 0.5$, and the d electron band dispersion $\varepsilon_{d\mathbf{k}}$ in Eq. (8) is the same as that for the single-band Hubbard model on a square lattice. J in Eq. (11) is always positive in the charge-transfer regime. Thus, $\mathcal{H}_{\text{ex}}$ in Eq. (12) describes the transverse component of the antiferromagnetic exchange interaction between the d and p electrons, while the longitudinal component of this interaction narrows the bandwidth of $\varepsilon_{\alpha\beta\mathbf{k}}$ in Eq. (9) from t to $t - Jn_d$. Further, $\mathcal{H}_{\text{ex}}$ indicates that the p electron is affected by the spin fluctuation of the d electron. As will be shown later, the d-wave superconducting gap composed of d and p electrons emerges from $\mathcal{H}_{\text{ex}}$. $\mathcal{H}_{\text{pair}}$ in Eq. (13) appears for the first time by considering the double occupancy of Cu sites. The pair-hopping term is not included in the single-band t–J model if double occupancy is excluded. In the model that includes the pair-hopping interaction, electrons favour pair formation [26]. This is also true in the presence of the on-site interaction [27, 28] and in the zero-bandwidth limit [29]. Thus, the pair-hopping term in my model is expected to provide superconductivity in another way.

I introduce another assumption according to the speculation about the ground state of the three-band Hubbard model [30]. In the normal ground state, the d and p electrons should be combined to construct coherent quasi-particles through hybridization. The matrix elements of the hybridization between the d and p electrons can be found in the components with $\mathbf{q} = \mathbf{0}$ in Eqs. (12) and (13) as follows. Defining

$$h_{pd} = -\frac{\mathrm{i}}{N} \sum_{\alpha} \sum_{\mathbf{k}} \left[v_{\alpha\mathbf{k}} \langle p_{\mathbf{k}\uparrow}^{\alpha\dagger} d_{\mathbf{k}\uparrow} \rangle_0 - v_{\alpha\mathbf{k}}^* \langle d_{\mathbf{k}\uparrow}^{\dagger} p_{\mathbf{k}\uparrow}^{\alpha} \rangle_0 \right] = -\frac{\mathrm{i}}{N} \sum_{\alpha} \sum_{\mathbf{k}} \left[v_{\alpha\mathbf{k}} \langle p_{\mathbf{k}\downarrow}^{\alpha\dagger} d_{\mathbf{k}\downarrow} \rangle_0 - v_{\alpha\mathbf{k}}^* \langle d_{\mathbf{k}\downarrow}^{\dagger} p_{\mathbf{k}\downarrow}^{\alpha} \rangle_0 \right], \tag{15}$$

$\mathcal{H}_{\text{eff}}$ can be rewritten as

$$\mathcal{H}_{\text{eff}} = \mathcal{H}_0' + \mathcal{H}_{\text{ex}}' + \mathcal{H}_{\text{pair}}' + \mathcal{H}_U', \tag{16}$$

where

$$\mathcal{H}_0' = \mathcal{H}_{\text{HF}} + \mathrm{i}Jh_{pd} \sum_{\alpha} \sum_{\mathbf{k}\sigma} \left(v_{\alpha\mathbf{k}} p_{\mathbf{k}\sigma}^{\alpha\dagger} d_{\mathbf{k}\sigma} - v_{\alpha\mathbf{k}}^* d_{\mathbf{k}\sigma}^{\dagger} p_{\mathbf{k}\sigma}^{\alpha} \right). \tag{17}$$

Here, $\langle A \rangle_0$ in Eq. (15) means the expectation value of A in the ground state of $\mathcal{H}'_0$. $\mathcal{H}'_{\text{ex}}$ and $\mathcal{H}'_{\text{pair}}$ indicate the exchange interaction and pair-hopping terms excluding the component with $\mathbf{q} = \mathbf{0}$ from Eqs. (12) and (13), respectively. Thus, in the ground state of $\mathcal{H}'_0$, the d and p electrons are combined to construct the coherent quasi-particles when $h_{pd} > 0$.

Hereafter, I treat $\mathcal{H}'_0$ as the unperturbed part of $\mathcal{H}_{\text{eff}}$ on the assumption that $h_{pd} > 0$. I diagonalize $\mathcal{H}'_0$ and derive the unperturbed Green functions as follows:

$$G^0_{dd}(\mathbf{k}, i\epsilon_n) = \frac{i\epsilon_n + \mu - \varepsilon_{xx\mathbf{k}} - \varepsilon_{yy\mathbf{k}}}{(i\epsilon_n + \mu - \varepsilon_{\mathbf{k}}^+)(i\epsilon_n + \mu - \varepsilon_{\mathbf{k}}^-)}, \tag{18}$$

$$G^0_{d\alpha}(\mathbf{k}, i\epsilon_n) = \frac{iJh_{pd}v_{\alpha\mathbf{k}}}{(i\epsilon_n + \mu - \varepsilon_{\mathbf{k}}^+)(i\epsilon_n + \mu - \varepsilon_{\mathbf{k}}^-)}, \tag{19}$$

$$G^0_{\alpha d}(\mathbf{k}, i\epsilon_n) = \frac{-iJh_{pd}v_{\alpha\mathbf{k}}^*}{(i\epsilon_n + \mu - \varepsilon_{\mathbf{k}}^+)(i\epsilon_n + \mu - \varepsilon_{\mathbf{k}}^-)}, \tag{20}$$

and

$$\begin{pmatrix} G^0_{xx}(\mathbf{k}, i\epsilon_n) & G^0_{xy}(\mathbf{k}, i\epsilon_n) \\ G^0_{yx}(\mathbf{k}, i\epsilon_n) & G^0_{yy}(\mathbf{k}, i\epsilon_n) \end{pmatrix} = \frac{1}{(i\epsilon_n + \mu)(i\epsilon_n + \mu - \varepsilon_{\mathbf{k}}^+)(i\epsilon_n + \mu - \varepsilon_{\mathbf{k}}^-)}$$
$$\times \begin{pmatrix} (i\epsilon_n + \mu - \varepsilon_{d\mathbf{k}})(i\epsilon_n + \mu - \varepsilon_{yy\mathbf{k}}) - J^2h_{pd}^2 v_{y\mathbf{k}}v_{y\mathbf{k}}^* & (i\epsilon_n + \mu - \varepsilon_{d\mathbf{k}})\varepsilon_{yx\mathbf{k}} + J^2h_{pd}^2 v_{y\mathbf{k}}v_{x\mathbf{k}}^* \\ (i\epsilon_n + \mu - \varepsilon_{d\mathbf{k}})\varepsilon_{xy\mathbf{k}} + J^2h_{pd}^2 v_{x\mathbf{k}}v_{y\mathbf{k}}^* & (i\epsilon_n + \mu - \varepsilon_{d\mathbf{k}})(i\epsilon_n + \mu - \varepsilon_{xx\mathbf{k}}) - J^2h_{pd}^2 v_{x\mathbf{k}}v_{x\mathbf{k}}^* \end{pmatrix}. \tag{21}$$

Here, I use the fermion Matsubara frequencies, $\epsilon_n = \pi T(2n + 1)$, with integer n and temperature T. μ is the chemical potential and

$$\varepsilon_{\mathbf{k}}^\pm = \frac{\varepsilon_{d\mathbf{k}} + \varepsilon_{xx\mathbf{k}} + \varepsilon_{yy\mathbf{k}}}{2} \pm \sqrt{\left(\frac{\varepsilon_{d\mathbf{k}} - \varepsilon_{xx\mathbf{k}} - \varepsilon_{yy\mathbf{k}}}{2}\right)^2 + J^2h_{pd}^2\left(v_{x\mathbf{k}}v_{x\mathbf{k}}^* + v_{y\mathbf{k}}v_{y\mathbf{k}}^*\right)}. \tag{22}$$

For $h_{pd} > 0$, Eq. (15) can be rewritten as

$$1 = \frac{2J}{N}\sum_{\mathbf{k}} \frac{v_{x\mathbf{k}}v_{x\mathbf{k}}^* + v_{y\mathbf{k}}v_{y\mathbf{k}}^*}{\varepsilon_{\mathbf{k}}^+ - \varepsilon_{\mathbf{k}}^-}\left\{\theta(\varepsilon_{\mathbf{k}}^+ - \mu) - \theta(\varepsilon_{\mathbf{k}}^- - \mu)\right\}, \tag{23}$$

where $\theta(x)$ means the Heaviside step function.

In order to investigate the superconductivity in a strong coupling framework, I start with the Dyson-Gor'kov equations:

$$G_{\mu\nu}(\mathbf{k}, i\epsilon_n) = G^0_{\mu\nu}(\mathbf{k}, i\epsilon_n) + G^0_{\mu\kappa}(\mathbf{k}, i\epsilon_n)\Sigma_{\kappa\lambda}(\mathbf{k}, i\epsilon_n)G_{\lambda\nu}(\mathbf{k}, i\epsilon_n) + G^0_{\mu\kappa}(\mathbf{k}, i\epsilon_n)\Phi_{\kappa\lambda}(\mathbf{k}, i\epsilon_n)F^\dagger_{\lambda\nu}(-\mathbf{k}, -i\epsilon_n), \tag{24}$$

$$F^\dagger_{\mu\nu}(\mathbf{k}, i\epsilon_n) = G^0_{\mu\kappa}(\mathbf{k}, i\epsilon_n)\Sigma_{\kappa\lambda}(\mathbf{k}, i\epsilon_n)F^\dagger_{\lambda\nu}(\mathbf{k}, i\epsilon_n) + G^0_{\mu\kappa}(\mathbf{k}, i\epsilon_n)\Phi^*_{\kappa\lambda}(\mathbf{k}, i\epsilon_n)G_{\lambda\nu}(-\mathbf{k}, -i\epsilon_n), \tag{25}$$

$$F_{\mu\nu}(\mathbf{k}, i\epsilon_n) = G^0_{\mu\kappa}(\mathbf{k}, i\epsilon_n)\Sigma_{\kappa\lambda}(\mathbf{k}, i\epsilon_n)F_{\lambda\nu}(\mathbf{k}, i\epsilon_n) + G^0_{\mu\kappa}(\mathbf{k}, i\epsilon_n)\Phi_{\kappa\lambda}(\mathbf{k}, i\epsilon_n)G_{\lambda\nu}(-\mathbf{k}, -i\epsilon_n). \tag{26}$$

The orbital indices μ, ν, κ, and λ run over d, x, and y, and I adopt the Einstein summation convention. $G_{\mu\nu}(\mathbf{k}, i\epsilon_n)$ and $F_{\mu\nu}(\mathbf{k}, i\epsilon_n)$ represent the normal and anomalous Green functions, respectively, and $\Sigma_{\mu\nu}(\mathbf{k}, i\epsilon_n)$ and $\Phi_{\mu\nu}(\mathbf{k}, i\epsilon_n)$ correspond to the normal and anomalous self-energies, respectively. When $\mathcal{H}'_{\text{ex}} + \mathcal{H}'_{\text{pair}} + \mathcal{H}'_U$ in Eq. (16) is treated as

a perturbation, the normal self-energies up to the second order of J and U are evaluated by the IPT approximation as follows:

$$\Sigma_{dd}(\mathbf{k}, i\epsilon_n) = \frac{T}{N} \sum_{\mathbf{k}'n'} \left[J^2 \chi_J^G(\mathbf{k} - \mathbf{k}', i\epsilon_n - i\epsilon_{n'}) G_{pp}^0(\mathbf{k}', i\epsilon_{n'}) + U^2 \chi_U(\mathbf{k} - \mathbf{k}', i\epsilon_n - i\epsilon_{n'}) G_{dd}^0(\mathbf{k}', i\epsilon_{n'}) \right],$$

(27)

$$\Sigma_{d\alpha}(\mathbf{k}, i\epsilon_n) = -v_{\alpha\mathbf{k}}^* \frac{T}{N} \sum_{\mathbf{k}'n'} \left[J^2 \chi_J^G(\mathbf{k} - \mathbf{k}', i\epsilon_n - i\epsilon_{n'}) G_{pd}^0(\mathbf{k}', i\epsilon_{n'}) \right],$$

(28)

$$\Sigma_{\alpha d}(\mathbf{k}, i\epsilon_n) = -v_{\alpha\mathbf{k}} \frac{T}{N} \sum_{\mathbf{k}'n'} \left[J^2 \chi_J^G(\mathbf{k} - \mathbf{k}', i\epsilon_n - i\epsilon_{n'}) G_{dp}^0(\mathbf{k}', i\epsilon_{n'}) \right],$$

(29)

$$\Sigma_{\alpha\beta}(\mathbf{k}, i\epsilon_n) = v_{\alpha\mathbf{k}} v_{\beta\mathbf{k}}^* \frac{T}{N} \sum_{\mathbf{k}'n'} \left[J^2 \chi_J^G(\mathbf{k} - \mathbf{k}', i\epsilon_n - i\epsilon_{n'}) G_{dd}^0(\mathbf{k}', i\epsilon_{n'}) \right].$$

(30)

The IPT approximation was first applied in the study of the half-filled single-impurity Anderson model [31, 32], and it was adopted to solve the effective impurity model in the study of the $d = \infty$ Hubbard model [33, 34]. In these works, it was shown that the second order perturbation theory in large energy scale U could reproduce not only the coherent band but also the lower and upper incoherent bands. In a later section, it will be shown that my approach can reproduce similar band structure to be justified as the theory for the 2D three-band t–J–U model.

The anomalous self-energies up to the second order of J and U are evaluated as follows:

$$\Phi_{dd}(\mathbf{k}, i\epsilon_n) = -\frac{T}{N} \sum_{\mathbf{k}'n'} \left[\left\{ J + J^2 \chi_J^F(\mathbf{k} - \mathbf{k}', i\epsilon_n - i\epsilon_{n'}) \right\} F_{pp}(\mathbf{k}', i\epsilon_{n'}) + \left\{ U + U^2 \chi_U(\mathbf{k} - \mathbf{k}', i\epsilon_n - i\epsilon_{n'}) \right\} F_{dd}(\mathbf{k}', i\epsilon_{n'}) \right],$$

(31)

$$\Phi_{d\alpha}(\mathbf{k}, i\epsilon_n) = v_{\alpha-\mathbf{k}} \frac{T}{N} \sum_{\mathbf{k}'n'} \left[\left\{ J + J^2 \chi_J^F(\mathbf{k} - \mathbf{k}', i\epsilon_n - i\epsilon_{n'}) \right\} F_{pd}(\mathbf{k}', i\epsilon_{n'}) \right],$$

(32)

$$\Phi_{\alpha d}(\mathbf{k}, i\epsilon_n) = v_{\alpha\mathbf{k}} \frac{T}{N} \sum_{\mathbf{k}'n'} \left[\left\{ J + J^2 \chi_J^F(\mathbf{k} - \mathbf{k}', i\epsilon_n - i\epsilon_{n'}) \right\} F_{dp}(\mathbf{k}', i\epsilon_{n'}) \right],$$

(33)

$$\Phi_{\alpha\beta}(\mathbf{k}, i\epsilon_n) = -v_{\alpha\mathbf{k}} v_{\beta-\mathbf{k}} \frac{T}{N} \sum_{\mathbf{k}'n'} \left[\left\{ J + J^2 \chi_J^F(\mathbf{k} - \mathbf{k}', i\epsilon_n - i\epsilon_{n'}) \right\} F_{dd}(\mathbf{k}', i\epsilon_{n'}) \right].$$

(34)

Here, the orbital indices α and β run over x and y, and

$$\chi_J^G(\mathbf{q}, i\omega_m) = \chi_{dd,pp}^G(\mathbf{q}, i\omega_m) - \chi_{dp,dp}^G(\mathbf{q}, i\omega_m) - \chi_{pd,pd}^G(\mathbf{q}, i\omega_m) + \chi_{pp,dd}^G(\mathbf{q}, i\omega_m), \quad (35)$$

$$\chi_J^F(\mathbf{q}, i\omega_m) = \chi_{dd,pp}^F(\mathbf{q}, i\omega_m) - \chi_{dp,pd}^F(\mathbf{q}, i\omega_m) - \chi_{pd,dp}^F(\mathbf{q}, i\omega_m) + \chi_{pp,dd}^F(\mathbf{q}, i\omega_m), \quad (36)$$

$$\chi_U(\mathbf{q}, i\omega_m) = \chi_{dd,dd}^G(\mathbf{q}, i\omega_m) + \chi_{dd,dd}^F(\mathbf{q}, i\omega_m), \quad (37)$$

$$\chi_{\mu\nu,\kappa\lambda}^G(\mathbf{q}, i\omega_m) = -\frac{T}{N} \sum_{\mathbf{k}n} G_{\mu\nu}^0(\mathbf{q} + \mathbf{k}, i\omega_m + i\epsilon_n) G_{\kappa\lambda}^0(\mathbf{k}, i\epsilon_n), \quad (38)$$

$$\chi_{\mu\nu,\kappa\lambda}^F(\mathbf{q}, i\omega_m) = -\frac{T}{N} \sum_{\mathbf{k}n} F_{\mu\nu}(\mathbf{q} + \mathbf{k}, i\omega_m + i\epsilon_n) F_{\kappa\lambda}^\dagger(\mathbf{k}, i\epsilon_n), \quad (39)$$

$$G_{pp}^0(\mathbf{k}, i\epsilon_n) = \sum_{\alpha\beta} v_{\alpha\mathbf{k}}^* v_{\beta\mathbf{k}} G_{\alpha\beta}^0(\mathbf{k}, i\epsilon_n), \quad (40)$$

$$G_{dp}^0(\mathbf{k}, i\epsilon_n) = \sum_{\alpha} v_{\alpha\mathbf{k}} G_{d\alpha}^0(\mathbf{k}, i\epsilon_n), \quad (41)$$

$$G^0_{pd}(\mathbf{k}, i\epsilon_n) = \sum_\alpha v^*_{\alpha\mathbf{k}} G^0_{\alpha d}(\mathbf{k}, i\epsilon_n), \tag{42}$$

$$F_{pp}(\mathbf{k}, i\epsilon_n) = \sum_{\alpha\beta} v^*_{\alpha\mathbf{k}} v^*_{\beta-\mathbf{k}} F_{\alpha\beta}(\mathbf{k}, i\epsilon_n), \tag{43}$$

$$F_{dp}(\mathbf{k}, i\epsilon_n) = \sum_\alpha v^*_{\alpha-\mathbf{k}} F_{d\alpha}(\mathbf{k}, i\epsilon_n), \tag{44}$$

$$F_{pd}(\mathbf{k}, i\epsilon_n) = \sum_\alpha v^*_{\alpha\mathbf{k}} F_{\alpha d}(\mathbf{k}, i\epsilon_n), \tag{45}$$

$$F^\dagger_{pp}(\mathbf{k}, i\epsilon_n) = \sum_{\alpha\beta} v_{\alpha\mathbf{k}} v_{\beta-\mathbf{k}} F^\dagger_{\alpha\beta}(\mathbf{k}, i\epsilon_n), \tag{46}$$

$$F^\dagger_{dp}(\mathbf{k}, i\epsilon_n) = \sum_\alpha v_{\alpha-\mathbf{k}} F^\dagger_{d\alpha}(\mathbf{k}, i\epsilon_n), \text{ and} \tag{47}$$

$$F^\dagger_{pd}(\mathbf{k}, i\epsilon_n) = \sum_\alpha v_{\alpha\mathbf{k}} F^\dagger_{\alpha d}(\mathbf{k}, i\epsilon_n), \tag{48}$$

using the boson Matsubara frequencies, $\omega_m = 2m\pi T$ with integer m. In Eqs. (38) and (39), μ, ν, κ, and λ denote d or p, respectively. Note that n_d, t, h_{pd}, and the chemical potential μ must be determined self-consistently in the ground state of $\mathcal{H}'_0$ through Eqs. (8)–(10), (22), and (23). To this end, I approximate n_d by the number of d electrons in the ground state of $\mathcal{H}'_0$:

$$n_d = 2 - \frac{2}{N} \sum_\mathbf{k} \frac{1}{\varepsilon^+_\mathbf{k} - \varepsilon^-_\mathbf{k}} \left\{ (\varepsilon^+_\mathbf{k} - \varepsilon_{xx\mathbf{k}} - \varepsilon_{yy\mathbf{k}})\theta(\varepsilon^+_\mathbf{k} - \mu) - (\varepsilon^-_\mathbf{k} - \varepsilon_{xx\mathbf{k}} - \varepsilon_{yy\mathbf{k}})\theta(\varepsilon^-_\mathbf{k} - \mu) \right\}. \tag{49}$$

Specifically, I regard n_d as a given parameter and solve Eqs. (8)–(10), (22), (23), and (49) to determine t, h_{pd}, and the number of doped holes δ^0_h for the ground state of $\mathcal{H}'_0$, where

$$\delta^0_\mathrm{h} = \frac{2}{N} \sum_\mathbf{k} \left[\theta(\varepsilon^+_\mathbf{k} - \mu) + \theta(\varepsilon^-_\mathbf{k} - \mu) + \theta(-\mu) \right] - 1. \tag{50}$$

Once t, h_{pd}, and δ^0_h are determined for the ground state of $\mathcal{H}'_0$, I treat t, h_{pd}, and δ^0_h as temperature independent parameters, whose values do not change from those at $T = 0$. Then, Eqs. (8)–(48) are solved in a fully self-consistent manner to obtain $\Sigma_{\mu\nu}(\mathbf{k}, i\epsilon_n)$ and $\Phi_{\mu\nu}(\mathbf{k}, i\epsilon_n)$. To determine the transition temperature T_c, I perform these calculations in two steps. First, $\Sigma_{\mu\nu}(\mathbf{k}, i\epsilon_n)$ is calculated with $\Phi_{\mu\nu}(\mathbf{k}, i\epsilon_n) = 0$, and μ is self-consistently determined so that δ_h obtained from $G_{\mu\nu}(\mathbf{k}, i\epsilon_n)$ becomes equal to δ^0_h. In the first step, μ is correctly adjusted to compensate the temperature-dependent shift by $\Sigma_{\mu\nu}(\mathbf{k}, i\epsilon_n)$ with $\Phi_{\mu\nu}(\mathbf{k}, i\epsilon_n) = 0$. Here, $\delta_\mathrm{h} = n_{dh} + n_{ph} - 1$, where

$$n_{dh} = 2 - 2\frac{T}{N} \sum_{\mathbf{k}n} G_{dd}(\mathbf{k}, i\epsilon_n) e^{i\epsilon_n 0^+}, \tag{51}$$

$$n_{ph} = 4 - 2\frac{T}{N} \sum_{\mathbf{k}n} \left[G_{xx}(\mathbf{k}, i\epsilon_n) + G_{yy}(\mathbf{k}, i\epsilon_n) \right] e^{i\epsilon_n 0^+}, \tag{52}$$

and n_{dh} and n_{ph} are the number of d and p holes, respectively. Next, using the determined μ, fully self-consistent calculations are performed to obtain $\Sigma_{\mu\nu}(\mathbf{k}, i\epsilon_n)$ and $\Phi_{\mu\nu}(\mathbf{k}, i\epsilon_n)$. At this time, only the temperature-dependent shift by $\Phi_{\mu\nu}(\mathbf{k}, i\epsilon_n)$ is reflected in δ_h obtained from $G_{\mu\nu}(\mathbf{k}, i\epsilon_n)$. That is, if δ_h deviates from δ^0_h, $\Phi_{\mu\nu}(\mathbf{k}, i\epsilon_n) \neq 0$. Therefore, the temperature at which δ_h deviates from δ^0_h is T_c. Also in the second step, μ

can be self-consistently determined so that δ_h obtained from $G_{\mu\nu}(\mathbf{k}, i\epsilon_n)$ becomes equal to δ_h^0 with $\Phi_{\mu\nu}(\mathbf{k}, i\epsilon_n) \neq 0$. In this case, the temperature at which μ deviates from the value with $\Phi_{\mu\nu}(\mathbf{k}, i\epsilon_n) = 0$ is T_c, which is consistent with the temperature at which δ_h deviates from δ_h^0 with fixed μ.

3. Results and discussion

To perform the numerical calculations, I divide the FBZ into a 64×64 meshes and prepare 2048 or 4096 Matsubara frequencies. I commonly use $t_{pd} = 10000\,\mathrm{K}$ for my calculations, and here, I only consider the case $\varepsilon_d = -U/2$. For this case, we have $J = t_{pd}$ when $U = 8\,t_{pd}$. I find fully self-consistent solutions with $h_{pd} > 0$ in $\delta_h \geq 0.117$. The ones in $0.117 \leq \delta_h \leq 0.139$ have $\Phi_{\mu\nu}(\mathbf{k}, i\epsilon_n) = 0$ and the others in $0.166 \leq \delta_h \leq 0.285$ have $\Phi_{\mu\nu}(\mathbf{k}, i\epsilon_n) \neq 0$. The former solutions correspond to metallic phase and the latter to superconducting phase. Although I find other fully self-consistent solutions with $h_{pd} = 0$ in $\delta_h \leq 0.031$, which correspond to insulating phase, I cannot find any solutions in $0.031 < \delta_h < 0.117$. The absence of solutions in this doping range indicates that some of my assumptions break down. In particular, it is difficult to achieve the spatially uniform distribution of the d electron in this range. For instance, the chemical potential shift suppression is observed in $\mathrm{La}_{2-x}\mathrm{Sr}_x\mathrm{CuO}_4$ ($0 < x < 0.12$) by photoemission spectroscopy [35, 36]. This suppression suggests the possibility of electronic phase separation between the insulating phase and the superconducting phase [37], where the electrons are inhomogeneously distributed due to the strong electron correlation. Therefore, the theory in $0.031 < \delta_h < 0.117$ should consider the possibility of the spatially non-uniform distribution of the d electron.
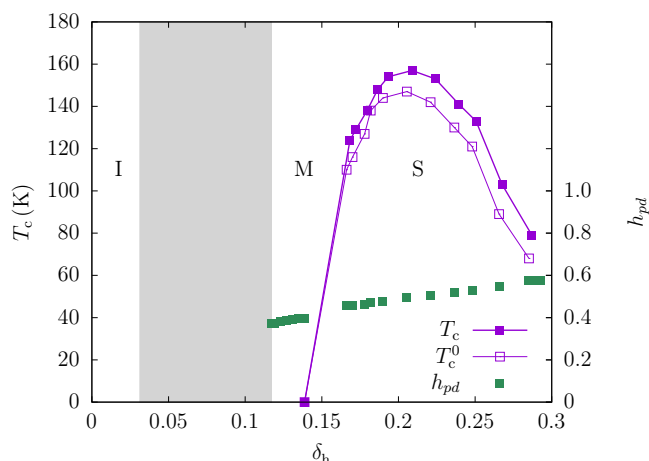

Figure 1. Doping dependences of T_c and h_{pd}. "I", "M" and "S" indicate insulating, metallic and superconducting phases, respectively. The shaded region indicates $0.031 < \delta_h < 0.117$ in which any solutions cannot be found. T_c^0 is the temperature at which the divergence of the Cooper susceptibility occurs. δ_h for T_c^0 and h_{pd} are evaluated at $T = 170\,\mathrm{K}$.

Figure 1 summarizes these results with the doping dependences of T_c and h_{pd}. Comparing T_c with T_c^0, at which the divergence of the Cooper susceptibility occurs, T_c

is higher than T_c^0 by $10 \sim 14\,\mathrm{K}$ since T_c reflects the fluctuation of $\Phi_{\mu\nu}(\mathbf{k}, i\epsilon_n)$. While h_{pd} increases monotonically with δ_h, T_c reaches its maximum, $157\,\mathrm{K}$, at $\delta_h = 0.209$ and then decreases. This doping dependence of T_c reproduces the dome-shaped superconducting phase that is typical for the hole-doped HTSC [38, 39]. This behavior is related to the doping dependence of the density of states, and it will be explained later.

Figure 2 shows the temperature dependences of $\delta_h - \delta_h^0$ for every δ_h^0, which are used to determine T_c. Here, I define the temperature at which $\delta_h - \delta_h^0$ jumps as T_c. The jumps of $\delta_h - \delta_h^0$ at T_c in the underdoped regime, $\delta_h^0 \leq 0.190$ [Fig. 2(a)], are larger than those in the overdoped regime, $\delta_h^0 \geq 0.205$ [Fig. 2(b)]. In other words, while strong coupling superconductivity is established in the underdoped regime, the superconductivity in the overdoped regime remains with weak coupling. This tendency must be reflected in the superconducting gap magnitude, which has been shown to decrease with doping by the low-temperature specific heats of $\mathrm{La}_{2-x}\mathrm{Sr}_x\mathrm{CuO}_4$ [40, 41].
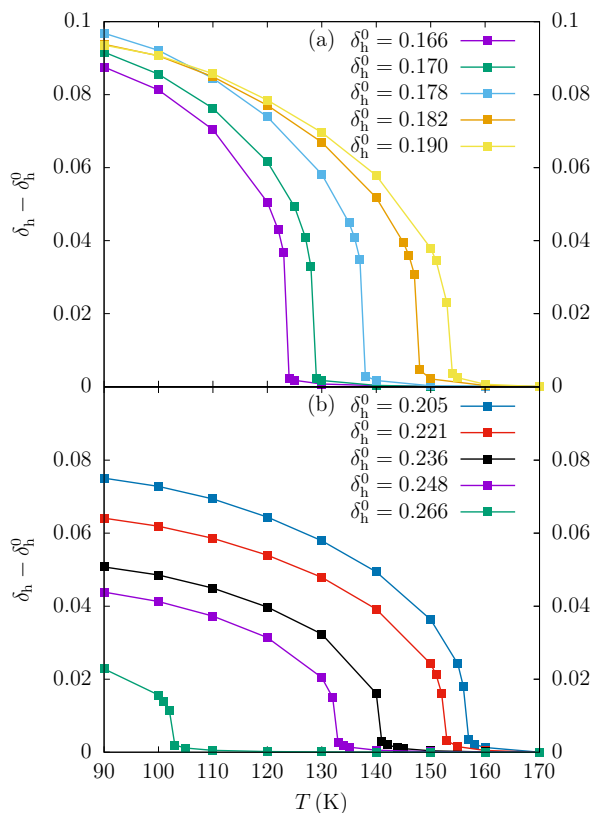

Figure 2. Temperature dependences of $\delta_h - \delta_h^0$: (a) $\delta_h^0 \leq 0.190$ and (b) $\delta_h^0 \geq 0.205$.

The electronic states of the obtained solutions are reconstructed from the unperturbed ground state. Figure 3 shows the doping dependences of n_{dh}, n_{ph}, n_{dh}^0, and n_{ph}^0 at $T = 170\,\mathrm{K}$. Here, $n_{dh}^0 = 2 - n_d$ and $n_{ph}^0 = \delta_h^0 + n_d - 1$, and n_{dh}^0 and n_{ph}^0 are the numbers of d and p holes in the unperturbed ground state, respectively. As shown in Fig. 3, holes are transferred from the d band to the p band due to the charge fluctuations $\chi_J^G(\mathbf{q}, i\omega_m)$ via the normal self-energies $\Sigma_{\mu\nu}(\mathbf{k}, i\epsilon_n)$ in Eqs. (27)–(30). As a consequence, while n_{ph} mainly increases with δ_h, $n_{dh} < 1$, which means that the d band is
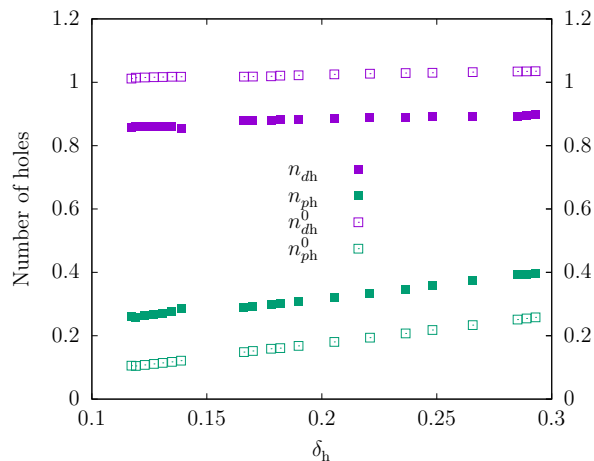
Figure 3. Doping dependences of n_{dh}, n_{ph}, n_{dh}^0, and n_{ph}^0 at $T = 170\,\mathrm{K}$.

always electron doped. Since the d band deviates from the half-filling due to the charge fluctuations, there is room for the pair-hopping interaction in Eq. (13) to work effectively between the p and d electrons despite the strong correlations among d electrons. Later, I show how the pair-hopping interaction works for the superconductivity in the analysis of the superconducting gap function.

Figures 4 and 5 show the doping dependences of $\rho_d(\varepsilon)$ and $\rho_p(\varepsilon)$ at $T = 170\,\mathrm{K}$, which elucidate how the dome-shaped superconducting phase develops. Here,

$$\rho_d(\varepsilon) = -\frac{1}{\pi N}\sum_{\mathbf{k}} \mathrm{Im}\, G_{dd}(\mathbf{k}, i\epsilon_n)|_{i\epsilon_n \to \varepsilon + i\eta}\,, \tag{53}$$

$$\rho_p(\varepsilon) = -\frac{1}{\pi N}\sum_{\mathbf{k}} \left[\mathrm{Im}\, G_{xx}(\mathbf{k}, i\epsilon_n)|_{i\epsilon_n \to \varepsilon + i\eta} + \mathrm{Im}\, G_{yy}(\mathbf{k}, i\epsilon_n)\Big|_{i\epsilon_n \to \varepsilon + i\eta}\right]. \tag{54}$$

$i\epsilon_n \to \varepsilon + i\eta$ indicates the performance of analytic continuation, for which I use the Padé approximation [42] and $\eta = 0.04\, t_{pd}$. $\rho_d(\varepsilon)$ and $\rho_p(\varepsilon)$ represent the density of states (DOS) of the d and p bands, respectively. It has been confirmed that the peak positions of $\rho_d(\varepsilon)$ and $\rho_p(\varepsilon)$ hardly change even if η is changed to $0.02\, t_{pd}$. The three blocks appearing in $\rho_d(\varepsilon)$ correspond to the lower Hubbard band, coherent band, and upper Hubbard band. The coherent band is split due to the hybridization with the p band, and the higher peak energy approaches the Fermi level with the hole doping [Fig. 5(a)]. In contrast, $\rho_p(\varepsilon)$ is large in the coherent band only. Reflecting that the holes are mainly doped into the p band, as shown in Fig. 3, the peak energy moves away from the Fermi level with the hole doping [Fig. 5(b)]. Due to the competitive effect of these changes in DOS in the coherent band, there is a dome-shaped superconducting phase.

The superconducting gap function, given in matrix form by $[\hat{\Delta}(\mathbf{k}, \varepsilon)]_{\mu\nu} \equiv \Delta_{\mu\nu}(\mathbf{k}, \varepsilon)$, is defined as follows:

$$\hat{\Delta}(\mathbf{k}, \varepsilon) = i\epsilon_n\, \mathrm{Im}\, \hat{G}(\mathbf{k}, i\epsilon_n) \cdot \hat{\Phi}(\mathbf{k}, i\epsilon_n)\Big|_{i\epsilon_n \to \varepsilon + i\eta}\,, \tag{55}$$

where $[\hat{G}(\mathbf{k}, i\epsilon_n)]_{\mu\nu} \equiv G_{\mu\nu}(\mathbf{k}, i\epsilon_n)$ and $[\hat{\Phi}(\mathbf{k}, i\epsilon_n)]_{\mu\nu} \equiv \Phi_{\mu\nu}(\mathbf{k}, i\epsilon_n)$. Here, I use the Padé approximation for analytic continuation and $\eta = 0.04\, t_{pd}$. It has been confirmed
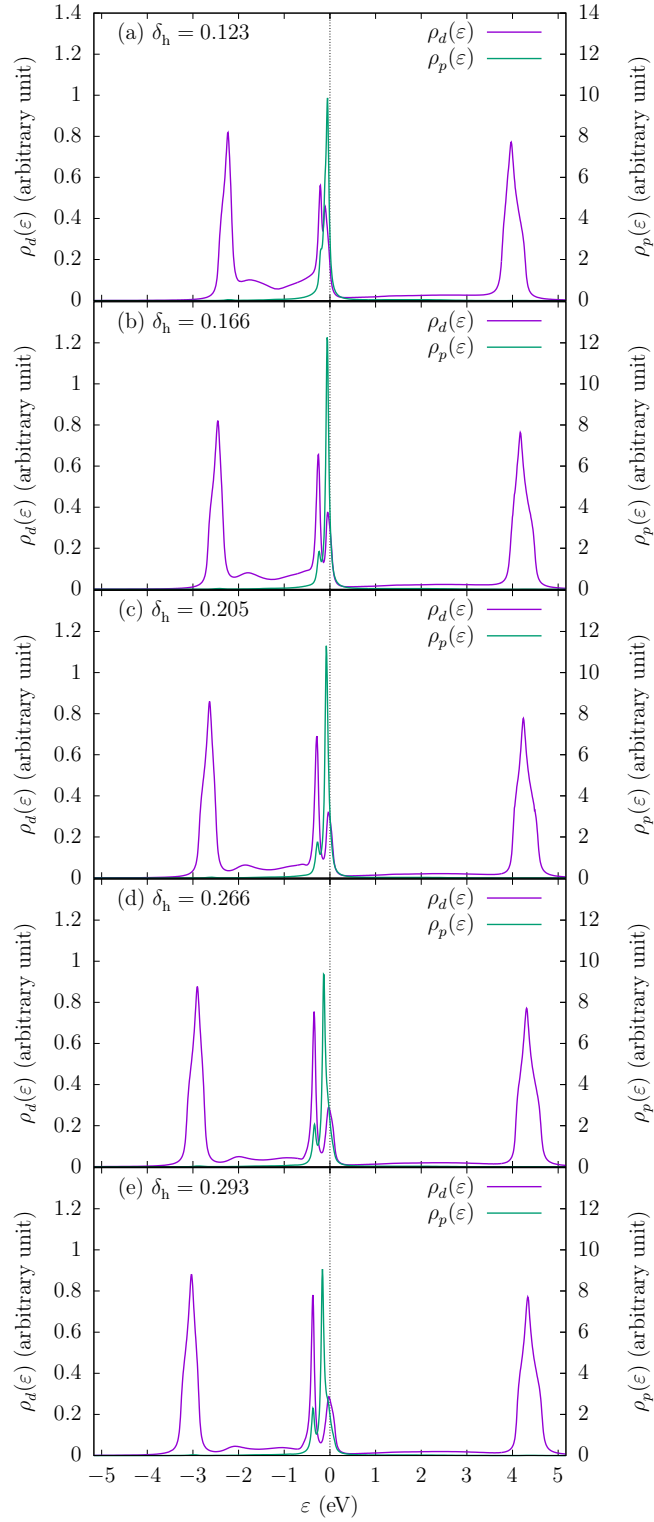
Figure 4. $\rho_d(\varepsilon)$ and $\rho_p(\varepsilon)$ at $T = 170\,\mathrm{K}$: (a) $\delta_\mathrm{h} = 0.123$, (b) $\delta_\mathrm{h} = 0.166$, (c) $\delta_\mathrm{h} = 0.205$, (d) $\delta_\mathrm{h} = 0.266$, and (e) $\delta_\mathrm{h} = 0.293$.
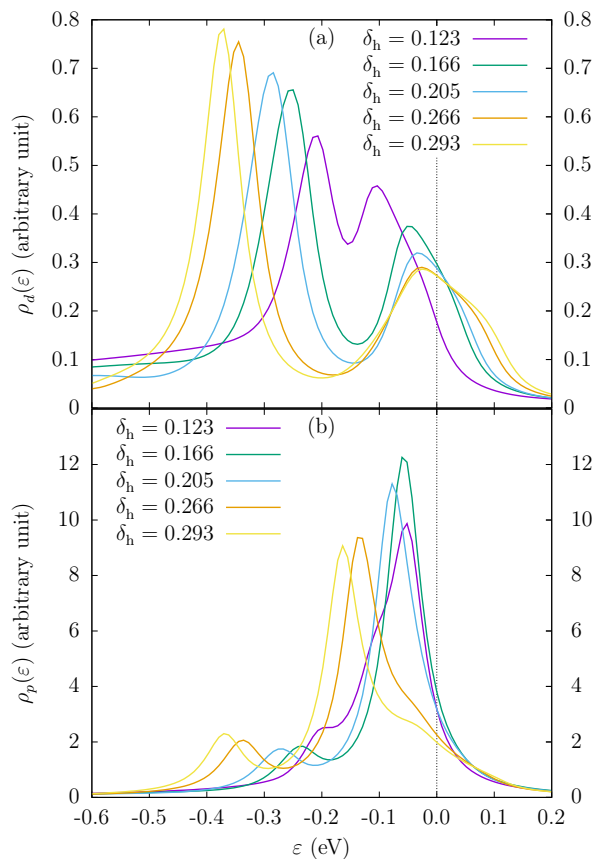
Figure 5. Doping dependences of $\rho_d(\varepsilon)$ and $\rho_p(\varepsilon)$ at $T = 170\,\mathrm{K}$ around the coherent band: (a) $\rho_d(\varepsilon)$ and (b) $\rho_p(\varepsilon)$.

that $\Delta_{\mu\nu}(\mathbf{k}, 0)$ hardly changes even if η is changed to $0.02\,t_{pd}$. The components of the superconducting gap function are classified into two classes. The first class is composed of $\Delta_{d\alpha}(\mathbf{k}, \varepsilon)$ and $\Delta_{\alpha d}(\mathbf{k}, \varepsilon)$, where α runs over x and y. The real parts of these components with $\varepsilon = 0$ are shown in Fig. 6. The imaginary parts of these components with $\varepsilon = 0$ are all zero. One can see that $\mathrm{Re}\Delta_{d\alpha}(\mathbf{k}, 0)$ [Fig. 6(a)] and $\mathrm{Re}\Delta_{\alpha d}(\mathbf{k}, 0)$ [Fig. 6(b)] are roughly proportional to $\sin\frac{k_\alpha}{2}$. These momentum dependences are derived from the first-order terms of J in Eqs. (32) and (33), which originate from the exchange interaction in Eq. (12). Thus, $\Delta_{d\alpha}(\mathbf{k}, \varepsilon)$ and $\Delta_{\alpha d}(\mathbf{k}, \varepsilon)$ emerge due to the exchange interaction via the SK mechanism. It can be verified that the SK mechanism can work effectively with the exchange interaction only if $h_{pd} > 0$. Moreover, the signs of $\mathrm{Re}\Delta_{dy}(\mathbf{k}, 0)$ and $\mathrm{Re}\Delta_{yd}(\mathbf{k}, 0)$ differ from the signs of $\mathrm{Re}\Delta_{dx}(\mathbf{k}, 0)$ and $\mathrm{Re}\Delta_{xd}(\mathbf{k}, 0)$, respectively. Therefore, as shown in Fig. 6(c), the linear combination $\mathrm{Re}\{\Delta_{dx}(\mathbf{k}, 0) + \Delta_{dy}(\mathbf{k}, 0) + \Delta_{xd}(\mathbf{k}, 0) + \Delta_{yd}(\mathbf{k}, 0)\}$ has line nodes at $k_x = k_y$ and $k_x = -k_y$ and behaves like a nodal $d_{x^2-y^2}$-wave superconducting gap.

The second class is composed of $\Delta_{dd}(\mathbf{k}, \varepsilon)$ and $\Delta_{\alpha\beta}(\mathbf{k}, \varepsilon)$, where α and β run over x and y. The real part of these components with $\varepsilon = 0$ are shown in Fig. 7. The imaginary part of these components with $\varepsilon = 0$ are all zero. $\mathrm{Re}\Delta_{\alpha\beta}(\mathbf{k}, 0)$ [Fig. 7(b) and (c)] is roughly proportional to $\sin\frac{k_\alpha}{2}\sin\frac{k_\beta}{2}$. This momentum dependence is derived
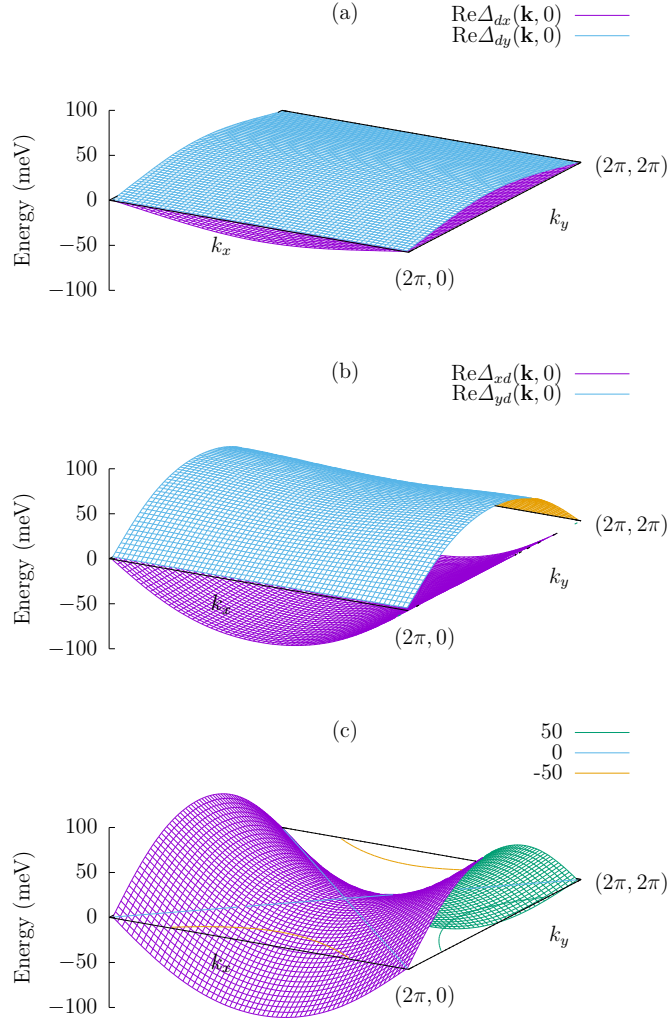
Figure 6. $\Delta_{d\alpha}(\mathbf{k}, 0)$ and $\Delta_{\alpha d}(\mathbf{k}, 0)$ at $\delta_{\mathrm{h}} = 0.237$ and $T = 110\,\mathrm{K}$: (a) $\mathrm{Re}\Delta_{dx}(\mathbf{k}, 0)$ and $\mathrm{Re}\Delta_{dy}(\mathbf{k}, 0)$, (b) $\mathrm{Re}\Delta_{xd}(\mathbf{k}, 0)$ and $\mathrm{Re}\Delta_{yd}(\mathbf{k}, 0)$, and (c) $\mathrm{Re}\{\Delta_{dx}(\mathbf{k}, 0) + \Delta_{dy}(\mathbf{k}, 0) + \Delta_{xd}(\mathbf{k}, 0) + \Delta_{yd}(\mathbf{k}, 0)\}$.

from the first-order term of J in Eq. (34), which originates from the pair-hopping interaction in Eq. (13). $\mathrm{Re}\Delta_{dd}(\mathbf{k}, 0)$ [Fig. 7(a)] has the momentum dependence of an extended s-wave, and its sign differs from the signs of $\mathrm{Re}\Delta_{xx}(\mathbf{k}, 0)$ and $\mathrm{Re}\Delta_{yy}(\mathbf{k}, 0)$. Thus, $\Delta_{dd}(\mathbf{k}, \varepsilon)$–as well as $\Delta_{\alpha\beta}(\mathbf{k}, \varepsilon)$–emerges due to the pair-hopping interaction via the SK mechanism, although it is affected by the terms of U and U^2 in Eq. (31). It can be verified that the SK mechanism can work with the pair-hopping interaction even if $h_{pd} = 0$. Moreover, the absolute values of $\mathrm{Re}\Delta_{dd}(\mathbf{k}, 0)$ are larger than those of $\mathrm{Re}\Delta_{\alpha\beta}(\mathbf{k}, 0)$ for all α, β, and $\mathbf{k}$. Therefore, as shown in Fig. 7(d), the linear combination $\mathrm{Re}\{\Delta_{dd}(\mathbf{k}, 0) + \Delta_{xx}(\mathbf{k}, 0) + \Delta_{xy}(\mathbf{k}, 0) + \Delta_{yx}(\mathbf{k}, 0) + \Delta_{yy}(\mathbf{k}, 0)\}$ behaves like an extended s-wave superconducting gap.

   I have shown that the coexistence of extended s- and d-wave gaps is theoretically
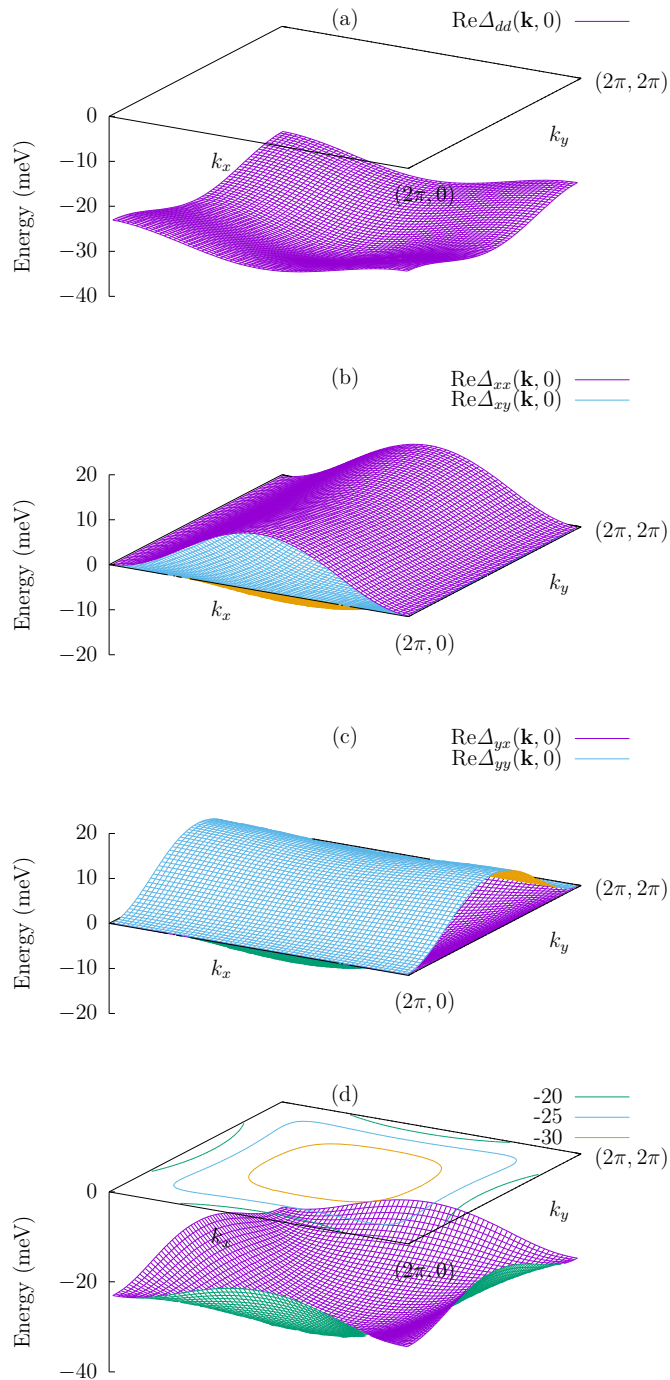
Figure 7. $\Delta_{dd}(\mathbf{k},0)$ and $\Delta_{\alpha\beta}(\mathbf{k},0)$ at $\delta_{\mathrm{h}} = 0.237$ and $T = 110\,\mathrm{K}$: (a) $\mathrm{Re}\Delta_{dd}(\mathbf{k},0)$, (b) $\mathrm{Re}\Delta_{xx}(\mathbf{k},0)$ and $\mathrm{Re}\Delta_{xy}(\mathbf{k},0)$, (b) $\mathrm{Re}\Delta_{yx}(\mathbf{k},0)$ and $\mathrm{Re}\Delta_{yy}(\mathbf{k},0)$, and (d) $\mathrm{Re}\{\Delta_{dd}(\mathbf{k},0) + \Delta_{xx}(\mathbf{k},0) + \Delta_{xy}(\mathbf{k},0) + \Delta_{yx}(\mathbf{k},0) + \Delta_{yy}(\mathbf{k},0)\}$.

possible in the three-band t–J–U model. The coexistence of s- and d-wave gaps was originally proposed to explain the apparently conflicting results of scanning tunnelling spectroscopy in HTSC [43]. So far, the experiments on $\mathrm{Bi_2Sr_2CaCu_2O_{8+\delta}}$ (Bi2212)

utilizing tunneling effect in the superconducting phase, which include c-axis twist Josephson experiments [44–50], c-axis scanning tunnelling microscopy [51–53], and intrinsic Josephson junction terahertz emission [54, 55], provide clear evidences that the superconducting gap has s-wave symmetry. These experiments can directly observe the superconducting gap without breaking the gap into quasiparticles, and this result is also reasonable for the coexistence of s- and d-wave gaps. In the superconducting phase, where s- and d-wave gaps coexist, the s-wave gap is dominant over the d-wave gap in the energy $|\varepsilon| < \Delta_s$, where Δ_s indicates the s-wave gap magnitude. On the other hand, only when the d-wave gap magnitude Δ_d satisfies $\Delta_d > \Delta_s$, the d-wave gap becomes dominant over the s-wave gap in the energy $|\varepsilon| > \Delta_s$.

In contrast, the quasiparticles from the d-wave gap can be observed in the energy $|\varepsilon| < \Delta_s$, where their excitation energies are always smaller than those of the quasiparticles from the s-wave gap. Thus, the experimental method breaking the gap into quasiparticles does mainly observe the d-wave gap. For example, both temperature and magnetic field dependences of low-temperature specific heat indicate that the d-wave superconducting gap exists in near optimally doped $Bi_2Sr_{2-x}La_xCuO_{6+\delta}$ ($x \sim 0.4$) [56].

The above discussion holds even if the d-wave gap is not a superconducting gap. The angle-resolved photoemission spectroscopy (ARPES) experiment on Bi2212 shows the marked change of temperature dependence of spectral intensity across critical value $p_c \sim 0.19$ with hole doping [57]. This change with hole doping p can be interpreted as a result of the coexistence of s- and d-wave gaps when we replace energy with temperature in the above discussion. For $p < p_c$, the d-wave gap affects the electronic structure above T_c if $\Delta_d > \Delta_s$. The electronic structure affected by the d-wave gap is called pseudogap. However, for $p > p_c$, both the s- and d-wave gaps do not affect the electronic structure above T_c if $\Delta_d < \Delta_s$. Therefore, the pseudogap disappears across p_c with hole doping, which has also been observed by the ARPES experiment [57].

Furthermore, Raman spectroscopy [58] and the magnetic field penetration depth measurement by muon-spin rotation [59–61] have provided evidence that supports the coexistence of s- and d-wave gaps in hole-doped HTSC. In theoretical work, the possibility of the coexistence of an extended s- and d-wave superconducting state has been shown with the analysis of the 2D t–J model considering fluctuation effects [13], and further experimental and theoretical research that assumes such coexistence is desired in the future.

I conclude by comparing the obtained superconducting state to that found in other theoretical work. The $d_{x^2-y^2}$-wave superconducting gap composed of $\Delta_{d\alpha}(\mathbf{k}, \varepsilon)$ and $\Delta_{\alpha d}(\mathbf{k}, \varepsilon)$, which emerges due to the exchange interaction via the SK mechanism, corresponds to the one mediated by antiferromagnetic spin fluctuations (AFSF) [62]. This is clear because the superexchange interaction among d electrons, which is responsible for the AFSF, can be derived from the exchange interaction between d and p electrons. In general, once the superexchange interaction acts between charge carriers, the $d_{x^2-y^2}$-wave superconductivity can emerge [63]. Moreover, the $d_{x^2-y^2}$-wave superconductivity in my model can emerge only with the d-p band hybridization.

Therefore, it must be important that the d electron is implicitly hybridized with the p electron in the AFSF-mediated superconductivity. This speculation is supported by the studies of Kondo lattice models proposed for copper oxide [64–71]. The Kondo interaction between localized d spin and p electron in Kondo lattice models corresponds to the exchange interaction between d and p electrons in the large-U limit of my model. The studies of Kondo lattice models indicate that superconductivity emerges due to the Kondo effect, the compensation for the localized d spin by the p electrons via the Kondo interaction. As the Kondo effect corresponds to the formation of a Fermi liquid state through the d-p band hybridization [30], the superconductivity in Kondo lattice models is consistent with the $d_{x^2-y^2}$-wave superconductivity in my model.

The extended s-wave superconducting gap composed of $\Delta_{dd}(\mathbf{k}, \varepsilon)$ and $\Delta_{\alpha\beta}(\mathbf{k}, \varepsilon)$, which emerges due to the pair-hopping interaction via the SK mechanism, corresponds to the kinetic-energy-driven superconductivity of the single-band t–J model [72–80]. In the kinetic-energy-driven superconductivity, the charge carriers form the superconducting pairs to gain kinetic energy. This energy gain can be derived from the pair-hopping interaction between p and d electrons, which works to form the extended s-wave superconducting gap in my model.

4. Summary

In summary, the three-band t–J–U model is derived assuming that the double occupancy by d electrons is not excluded. When the d electron is hybridized with the p electron through exchange and pair-hopping interactions, the dome-shaped superconducting phase can be reproduced despite the strong correlations among d electrons. In the superconducting phase, the extended s- and $d_{x^2-y^2}$-wave superconducting gaps coexist. The extended s-wave gap emerges due to the pair-hopping interaction via the SK mechanism, which works effectively due to the charge fluctuations. In contrast, the $d_{x^2-y^2}$-wave gap emerges due to the exchange interaction via the SK mechanism, which can effectively work only with the d-p band hybridization. The obtained superconducting state is consistent with those in other theoretical work, which include AFSF-mediated superconductivity and kinetic-energy-driven superconductivity.

Acknowledgements

References

[1] Chao K A, Spałek J and Oleś A M 1977 *J. Phys. C: Solid State Phys.* **10** L271
[2] Chao K A, Spałek J and Oleś A M 1978 *Phys. Rev.* B **18** 3453
[3] Zhang F C and Rice T M 1988 *Phys. Rev.* B **37** 3759

[4] Zaanen J and Oleś A M 1988 *Phys. Rev.* B **37** 9423
[5] Matsukawa H and Fukuyama H 1989 *J. Phys. Soc. Jpn.* **58** 2845
[6] Mori M, Tohyama T and Maekawa S 2002 *Phys. Rev.* B **66** 064502
[7] Plakida N M 2002 *Cond. Matter Phys.* **5** 707
[8] Rösch O and Gunnarsson O 2004 *Phys. Rev. Lett.* **92** 146403
[9] Ishihara S and Nagaosa N 2004 *Phys. Rev.* B **69** 144520
[10] Tohyama T 2004 *Phys. Rev.* B **70** 174517
[11] Mishchenko A S and Nagaosa N 2004 *Phys. Rev. Lett.* **93** 036402
[12] Mishchenko A S and Nagaosa N 2006 *Phys. Rev.* B **73** 092502
[13] Mallik Aabhaas V, Gupta Gaurav K, Shenoy Vijay B and Krishnamurthy H R 2020 *Phys. Rev. Lett.* **124** 147002
[14] Zhang F C 2003 *Phys. Rev. Lett.* **90** 207002
[15] Yuan F, Yuan Q and Ting C S 2005 *Phys. Rev.* B **71** 104505
[16] Wang Q H, Wang Z D, Chen Y and Zhang F C 2006 *Phys. Rev.* B **73** 092507
[17] Abram M, Kaczmarczyk J, Jędrak J and Spałek J 2013 *Phys. Rev.* B **88** 094502
[18] Spałek J, Zegrodnik M and Kaczmarczyk J 2017 *Phys. Rev.* B **95** 024506
[19] Zegrodnik M and Spałek J 2017 *Phys. Rev.* B **96** 054511
[20] Fidrysiak M and Spałek J 2020 *Phys. Rev.* B **102** 014505
[21] Schrieffer J R and Wolff P A 1966 *Phys. Rev.* **149** 491
[22] Suhl H, Matthias B T and Walker L R 1959 *Phys. Rev. Lett.* **3** 552
[23] Kondo J 1963 *Prog. Theor. Phys.* **29** 1
[24] Kondo J 2002 *J. Phys. Soc. Jpn.* **71** 1353
[25] Emery V J 1987 *Phys. Rev. Lett.* **58** 2794
[26] Penson K A and Kolb M 1986 *Phys. Rev.* B **33** 1663
[27] Belkasri A and Buzatu F D 1996 *Phys. Rev.* B **53** 7171
[28] Robaszkiewicz S and Bułka B D 1999 *Phys. Rev.* B **59** 6430
[29] Kapcia K J 2014 *Acta Phys. Pol. A* **126** 53
[30] Yamada K, Yosida K and Hanzawa K 1992 *Prog. Theor. Phys. Suppl.* No. 108 141
[31] Yamada K 1975 *Prog. Theor. Phys.* **53** 970
[32] Yosida K and Yamada K 1975 *Prog. Theor. Phys.* **53** 1286
[33] Georges A and Kotliar G 1992 *Phys. Rev.* B **45** 6479
[34] Zhang X Y, Rozenberg M J and Kotliar G 1993 *Phys. Rev. Lett.* **70** 1666
[35] Ino A, Mizokawa T, Fujimori A, Tamasaku K, Uchida S, Kimura T, Sasagawa T and Kishio K 1997 *Phys. Rev. Lett.* **79** 2101
[36] Fujimori A, Ino A, Mizokawa T, Kim C, Shen Z X, Sasagawa T, Kimura T, Kishio K, Takaba M, Tamasaku K, Eisaki H and Uchida S 1998 *J. Phys. Chem. Solids* **59** 1892
[37] Fujimori A, Ino A, Yoshida T, Mizokawa T, Shen Z X, Kim C, Kakeshita T, Eisaki H and Uchida S 2001, *Open Problems in Strongly Correlated Electron Systems* ed J. Bonca *et al.* (Dordrecht: KluIr Academic Pub.) p 119
[38] Tsukada A, Yamamoto H and Naito M 2006 *Phys. Rev.* B **74** 174515
[39] Yoshida T, Zhou X J, Tanaka K, Yang W L, Hussain Z, Shen Z X, Fujimori A, Sahrakorpi S, Lindroos M, Markiewicz R S, Bansil A, Komiya Seiki, Ando Yoichi, Eisaki H, Kakeshita T and Uchida S 2006 *Phys. Rev.* B **74** 224510
[40] Wen H-H, Shan L, Wen X G, Wang Y, Gao H, Liu Z Y, Zhou F, Xiong J W and Ti W X 2005 *Phys. Rev.* B **72** 134507
[41] Wang Y, Yan J, Shan L, Wen H-H, Tanabe Y, Adachi T and Koike Y 2007 *Phys. Rev.* B **76** 064512
[42] Vidberg H J and Serene J W 1977 *J. Low. Temp. Phys.* **29** 179
[43] Müller K A 1995 *Nature* **377** 133
[44] Li Qiang, Tsay Y N, Suenaga M, Klemm R A, Gu G D and Koshizuka N 1999 *Phys. Rev. Lett.* **83** 4160

[45] Takano Y, Hatano T, Fukuyo A, Ishii A, Ohmori M, Arisawa S, Togano K and Tachiki M 2002 *Phys. Rev.* B **65** 140513(R)

[46] Takano Y, Hatano T, Ohmori M, Kawakami S, Ishii A, Arisawa S, Kim S-J, Yamashita T, Togano K and Tachiki M 2003 *J. Low. Temp. Phys.* **131** 533

[47] Takano Y, Hatano T, Kawakami S, Ohmori M, Ikeda S, Nagao M, Inomata K, Yun K S, Ishii A, Tanaka A, Yamashita T and Tachiki M 2004 *Physica* C **408-410** 296

[48] Latyshev Y I, Orlov A P, Nikitina A M, Monceau P and Klemm R A 2004 *Phys. Rev.* B **70** 094517

[49] Klemm R A 2005 *Phil. Mag.* **85** 801

[50] Zhu Y, Liao M, Zhang Q, Xe H-Y, Meng F, Liu Y, Bai Z, Ji S, Zhang J, Jiang K, Zhong R, Schneeloch J, Gu G, Gu L, Ma X, Zhang D and Xue Q-K 2021 arXiv:1903.07965v2

[51] Misra S, Oh S, Hornbaker D J, DiLuccio T, Eckstein J N and Yazdani A 2002 *Phys. Rev. Lett.* **89** 087002

[52] Hoogenboom B W, Kadowaki K, Revaz B and Fischer Ø 2003 *Physica* C **391** 376

[53] Zhong Y, Wang Y, Han S, Lv Y-F, Wang W-L, Zhang D, Ding H, Zhang Y-M, Wang L, He K, Zhong R, Schneeloch J, Gu G-D, Song C-L, Ma X-C and Xue Q-K 2016 *Sci. Bull.* **61** 1239

[54] Kashiwagi T, Sakamoto K, Kubo H, Shibano Y, Enomoto T, Kitamura T, Asanuma K, Yasui T, Watanabe C, Nakade K, Saiwai Y, Katsuragawa T, Tsujimoto M, Yoshizaki R, Yamamoto T, Minami H, Klemm R A and Kadowaki K 2015 *Appl. Phys. Lett.* **107** 082601

[55] Kashiwagi T, Yamamoto T, Minami H, Tsujimoto M, Yoshizaki R, Delfanazari K, Kitamura T, Watanabe C, Nakade K, Yasui T, Asanuma K, Saiwai Y, Shibano Y, Enomoto T, Kubo H, Sakamoto K, Katsuragawa T, Marković B, Mirković J, Klemm R A and Kadowaki K 2015 *Phys. Rev. Appl.* **4** 054018

[56] Wang Y, Liu Z-Y, Lin C T and Wen H-H 2011 *Phys. Rev.* B **83** 054509

[57] Chen S-D, Hashimoto M, He Y, Song D, Xu K-J, He J-F, Devereaux T P, Eisaki H, Lu D-H, Zaanen J, Shen Z-X 2019 *Science* **366** 1099

[58] Masui T, Limonov M, Uchiyama H, Lee S, Tajima S and Yamanaka A 2003 *Phys. Rev.* B **68** 060506(R)

[59] Khasanov R, Shengelaya A, Maisuradze A, La Mattina F, Bussmann-Holder A, Keller H and Müller K A 2007 *Phys. Rev. Lett.* **98** 057007

[60] Khasanov R, Strässle S, Di Castro D, Masui T, Miyasaka S, Tajima S, Bussmann-Holder A and Keller H 2007 *Phys. Rev. Lett.* **99** 237601

[61] Khasanov R, Shengelaya A, Bussmann-Holder A, Karpinski J, Keller H and Müller K A 2008 *J. Supercond. Nov. Magn.* **21** 81

[62] Moriya T and Ueda K 2000 *Adv. Phys.* **49** 555 and references therein

[63] Que W-M and Kirczenow G 1987 *Solid State Commun.* **64** 1052

[64] Prelovšek P 1988 *Phys. Lett.* A **126** 287

[65] Ramšak A and Prelovšek P 1989 *Phys. Rev.* B **40** 2239

[66] Castellani C, Di Castro C and Grilli M 1988 *Physica* C **153-155** 1659

[67] Castellani C, Di Castro C and Grilli M 1988 *Int. J. Mod. Phys.* B **2** 659

[68] Cancrini N, Caprara S, Castellani C, Di Castro C, Grilli M and Raimondi R 1991 *Europhys. Lett.* **14** 597

[69] Kamimura H 1988 *Int. J. Mod. Phys.* B **2** 699

[70] Andrei N and Coleman P 1989 *Phys. Rev. Lett.* **62** 595

[71] Hatsugai Y, Imada M and Nagaosa N 1989 *J. Phys. Soc. Jpn.* **58** 1347

[72] Hirsch J E 1992 *Physica* C **201** 347

[73] Tsunetsugu H and Imada M 1998 *J. Phys. Soc. Jpn.* **67** 1864

[74] Tsunetsugu H and Imada M 1999 *J. Phys. Soc. Jpn.* **68** 3162

[75] Imada M and Onoda S 2001, *Open Problems in Strongly Correlated Electron Systems* ed J. Bonca *et al.* (Dordrecht: KluIr Academic Pub.) p 69

[76] Sarker S K and Lovorn T 2010 *Phys. Rev.* B **82** 014504

[77] Sarker S K and Lovorn T 2012 *Phys. Rev.* B **85** 144502
[78] Feng S, Zhao H and Huang Z 2012 *Phys. Rev.* B **85** 054509
[79] Feng S, Kuang L and Zhao H 2015 *Physica* C **517** 5
[80] Gao D, Mou Y and Feng S 2018 *J. Low Temp. Phys.* **192** 19